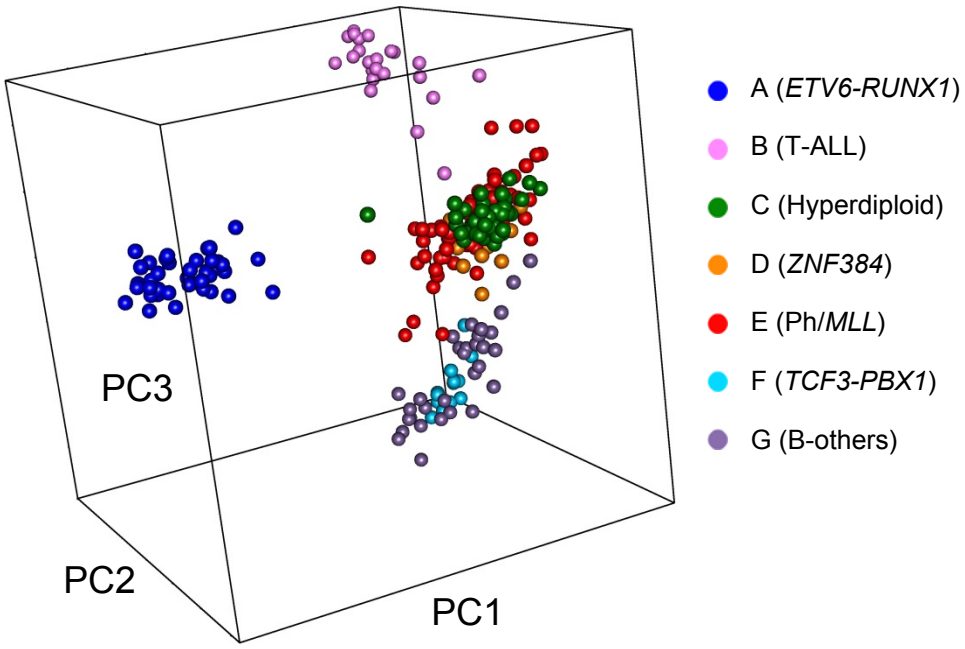

Supplemental Figure S1. Principal component analysis of ALL gene expression clusters. Each patient is represented by a sphere and color-coded to indicate the ALL subgroup to which it belongs in the Ma-Spore frontline ALL cohort.

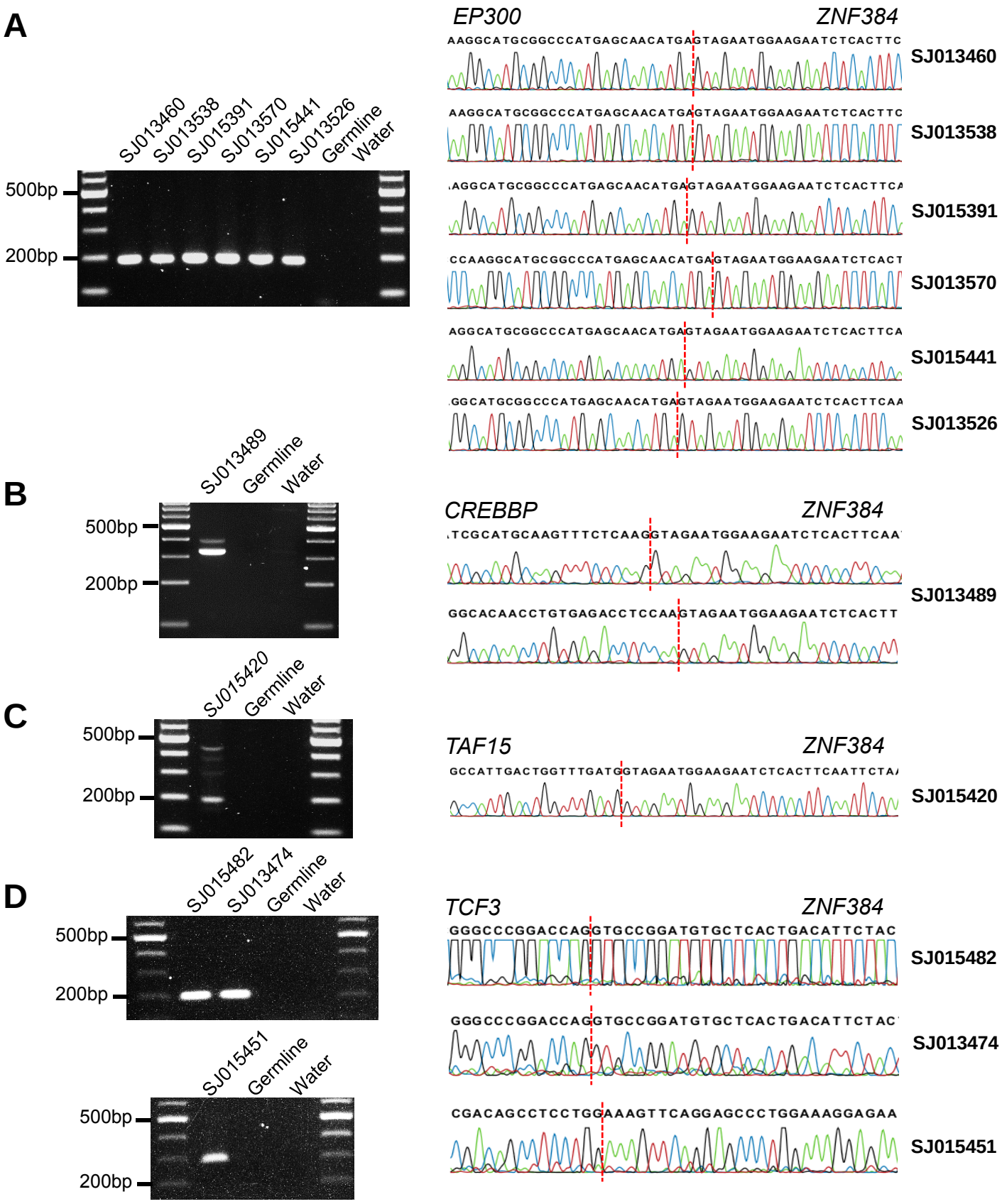

Supplemental Figure S2. Chromosome rearrangements involving *ZNF384*. For each type of *ZNF384* fusion observed (Panels A-D), fusion breakpoint region was amplified by RT-PCR from the corresponding patient sample and confirmed by Sanger sequencing. The cDNA from human cell line GM12878 (wildtype *ZNF384*) and water were use as negative and empty controls, respectively (Left Panels). Chromatogram shows sequencing results of the chimeric transcript with junction indicated by the dashed vertical line (Right Panels).

A

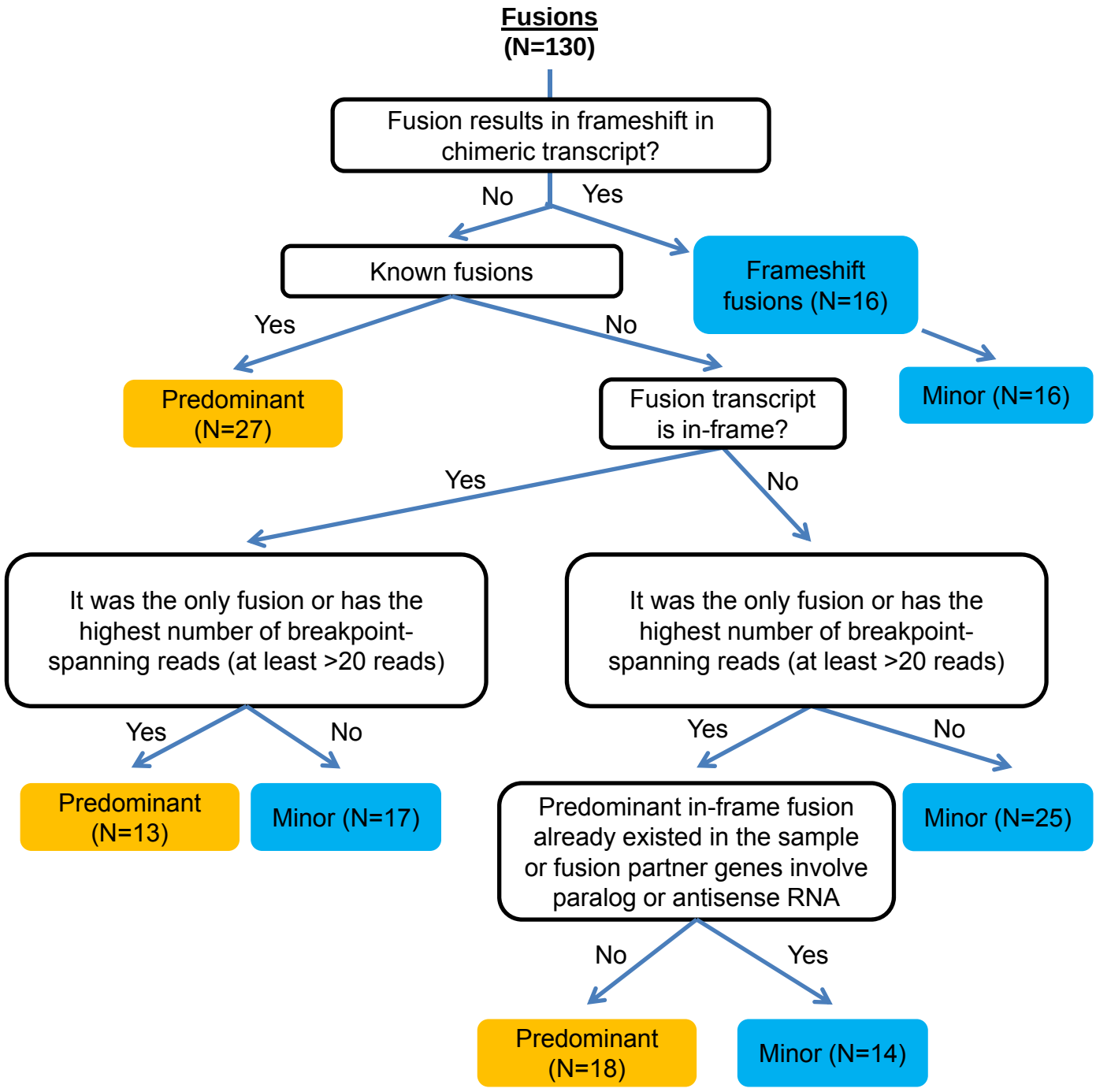
Fusions
(N=130)
Fusion results in frameshift in chimeric transcript?
No
Yes
Known fusions
Frameshift fusions (N=16)
Yes
No
Predominant (N=27)
Fusion transcript is in-frame?
Minor (N=16)
Yes
No
It was the only fusion or has the highest number of breakpoint-spanning reads (at least >20 reads)
It was the only fusion or has the highest number of breakpoint-spanning reads (at least >20 reads)
Yes
No
Yes
No
Predominant (N=13)
Minor (N=17)
Predominant in-frame fusion already existed in the sample or fusion partner genes involve paralog or antisense RNA
Minor (N=25)
No
Yes
Predominant (N=18)
Minor (N=14)

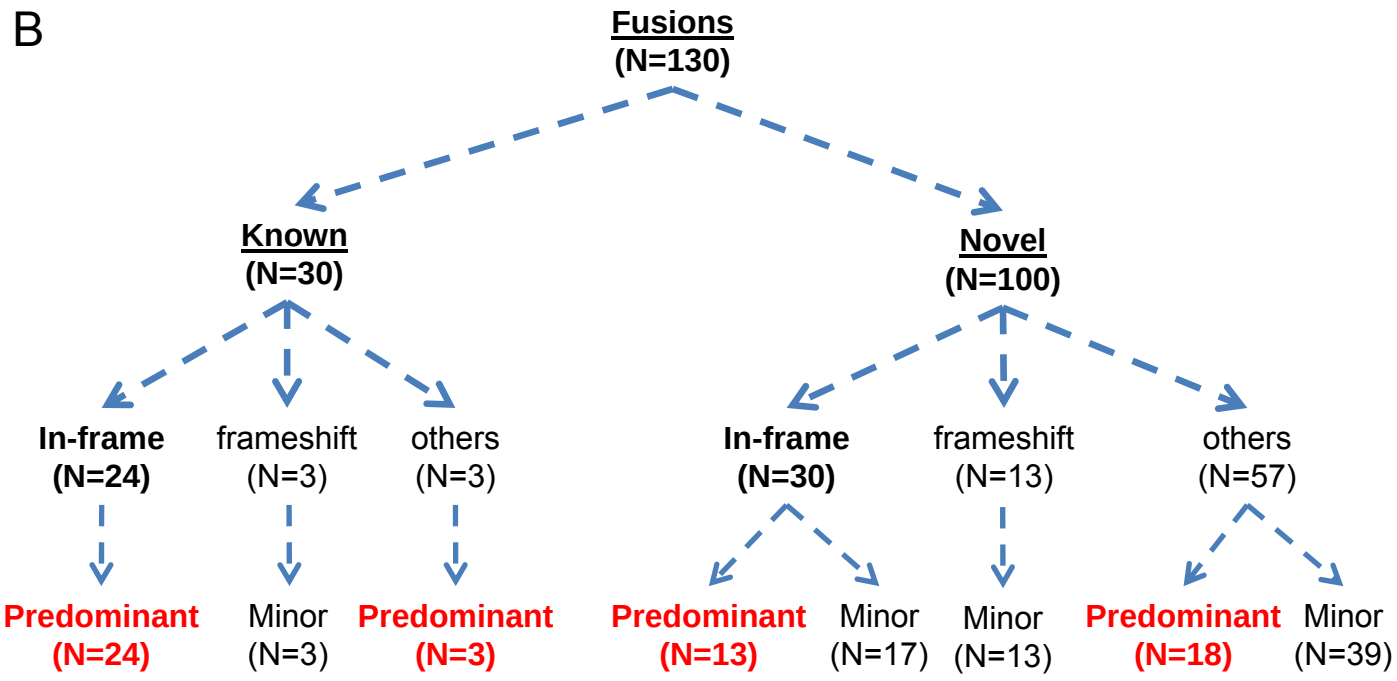

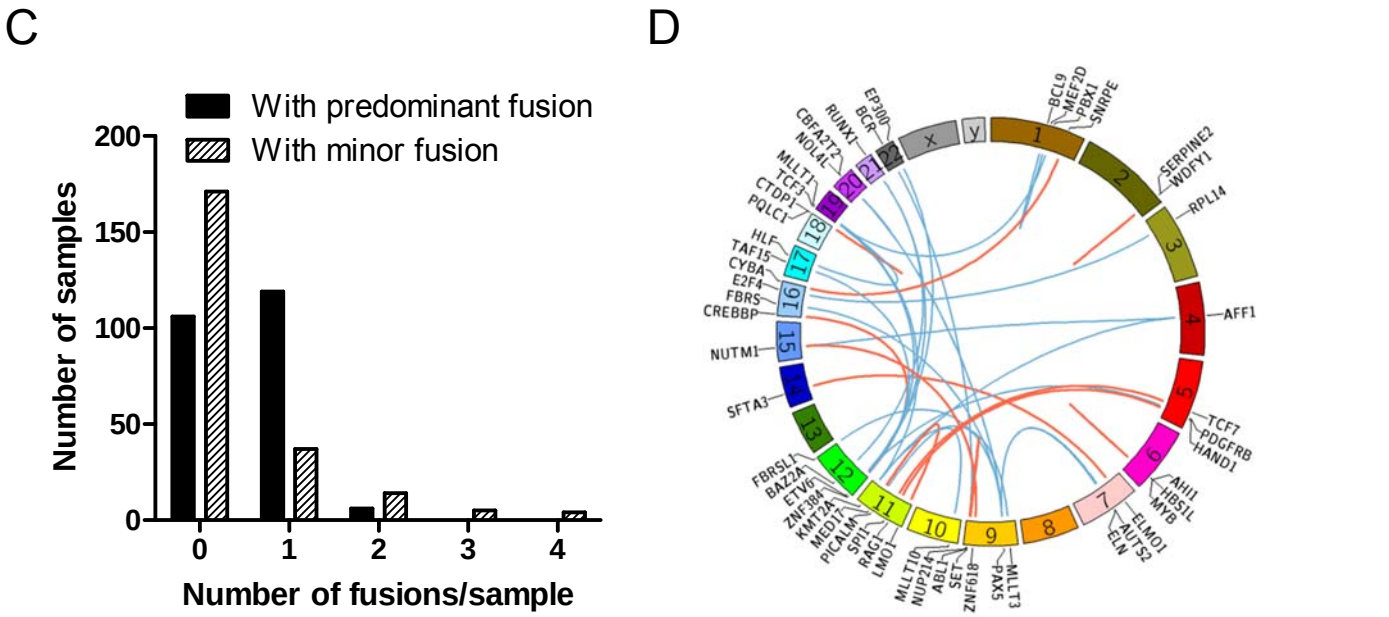

Supplemental Figure S3. Classification of ALL fusion genes identified from whole transcriptome sequencing. (A) Flow chart of the process to identify fusions as “predominant”, “minor”. (B) Enumeration of fusions that fall under each classes. (C) Distribution of the number of predominant vs. minor fusions per sample. (D) Circos plot of all predominant in-frame gene fusions (orange, novel fusion; blue, known fusion). The line links the two partner genes in a fusion.

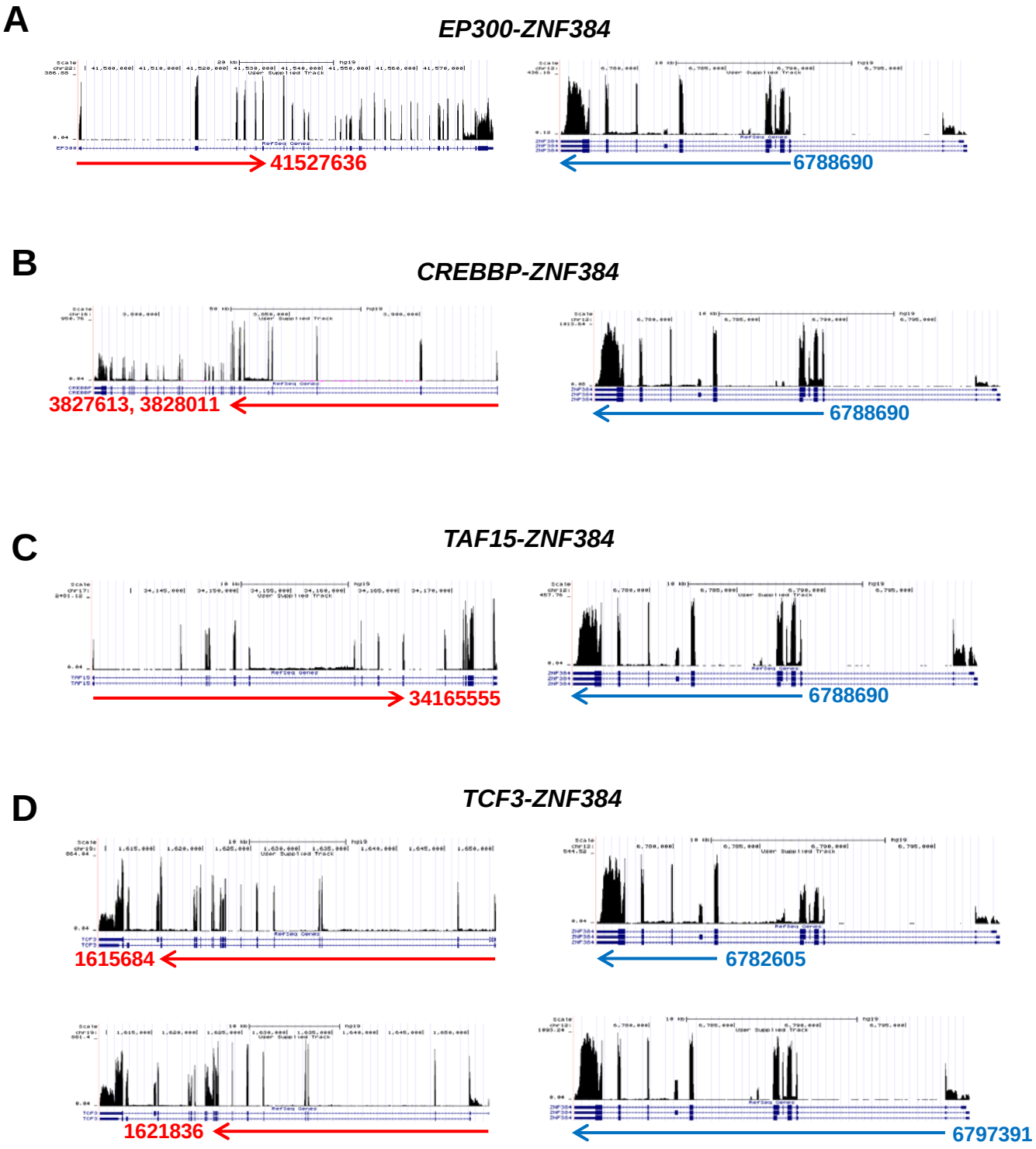

Supplemental Figure S4. Chromosome rearrangements involving *ZNF384*. For each type of *ZNF384* fusion observed (Panels A-D), RNA sequencing coverage for each partner gene is plotted across the genomic locus in genome browser with the arrows marking gene segments retained in chimeric transcript (blue and red for 5' and 3' partner genes, respectively). Fusion was amplified by RT-PCR from the corresponding patient sample and confirmed by Sanger sequencing (Supplemental Fig. S2).

A

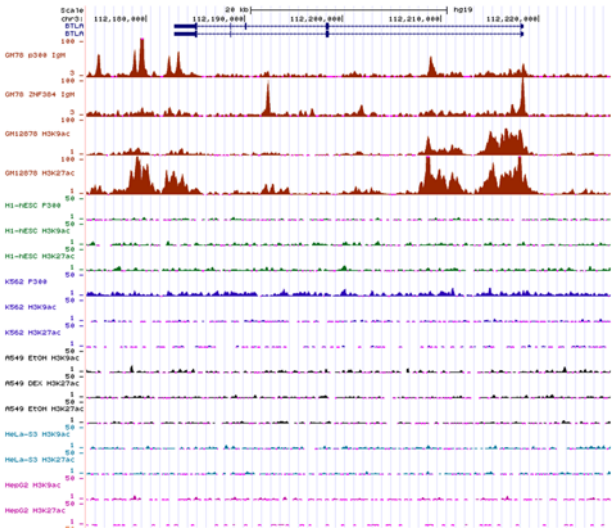

B

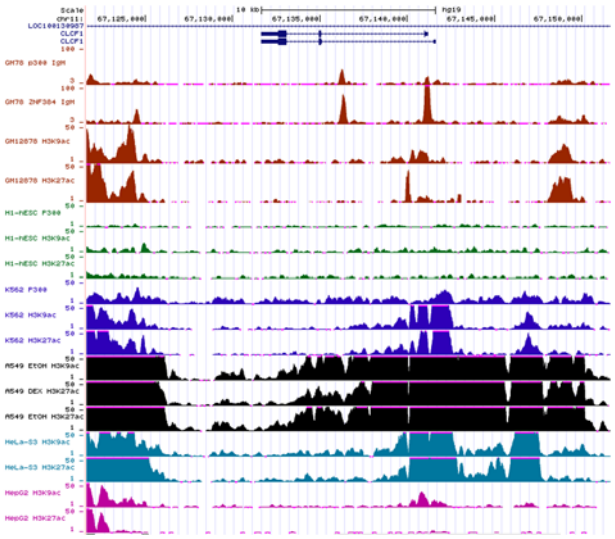

Supplemental Figure S5. ENCODE transcription factor and histone ChIP-seq at the *CLCF1* and *BTLA* loci. ZNF384 binding, EP300 binding, and histone modifications (H3K9ac and H3K27ac) as measured by ChIP-seq is plotted against the genome coordinates for the *BTLA* (A) and *CLCF1*(B) genes in human cell lines GM12878, H1-hESC, K562, A549, Hela-S3 and HepG2. Data was based on the ENCODE tracks in UCSC Genome Browser.

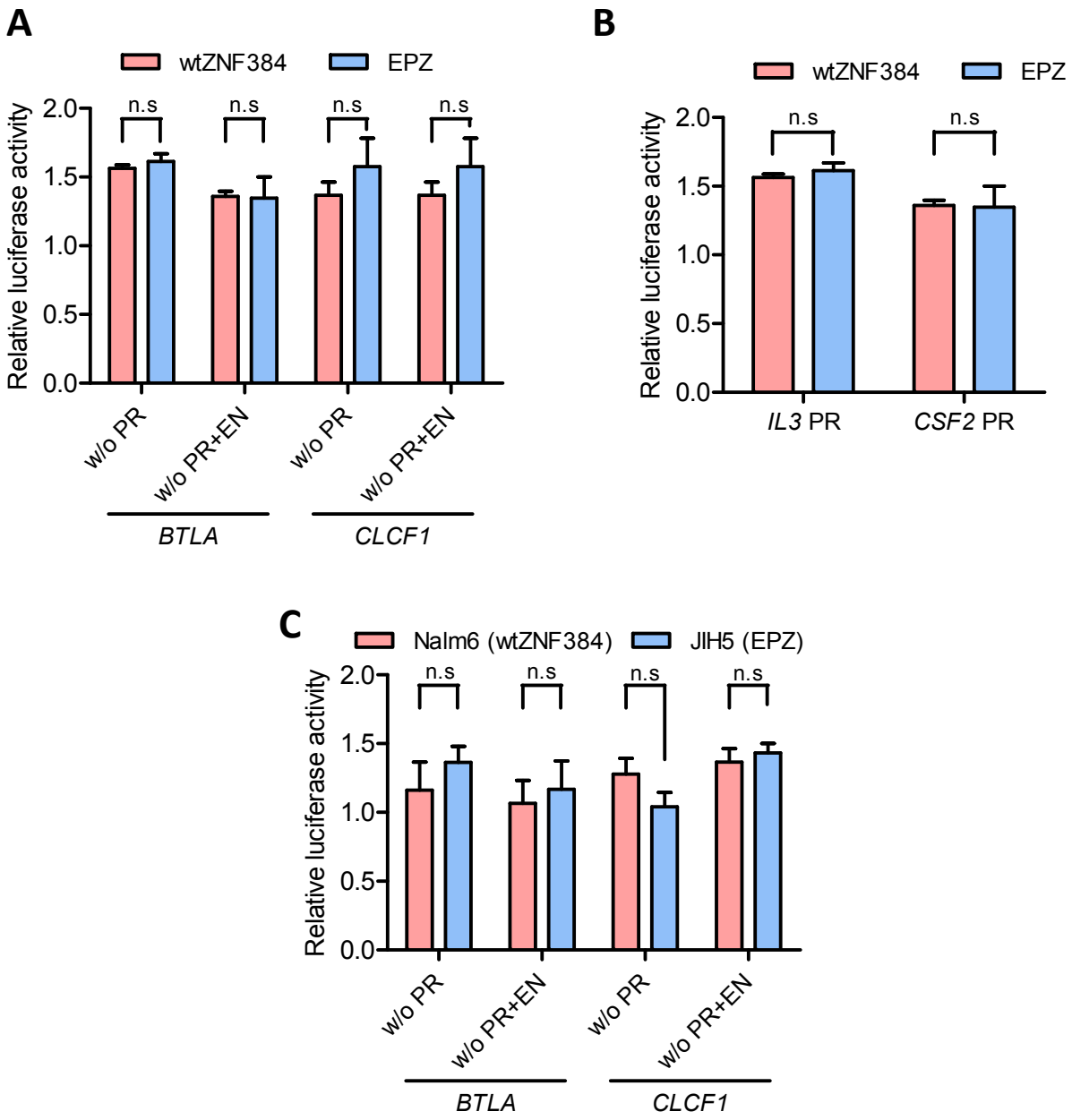

Supplemental Figure S6. *ZNF384* fusion did not affect promoter and enhancer activity in the absence of ZNF384-binding sequences. HEK293T cells were transiently transfected with pGL3 construct of luciferase gene downstream of 1) *BTLA* promoter void of ZNF384 binding sequence (i.e., *BTLA* w/o PR) or 2) *BTLA* promoter plus enhancer void of ZNF384 binding sequence [*BTLA* w/o PR+EN]). Luciferase activity was measured upon transduction with wildtype *ZNF384* [wt*ZNF384*] or *EP300-ZNF384* [EPZ]) in pcDNA vector and pGL-TK (Renilla luciferase). The same set of experiments were performed for *CLCF1* promoter and enhancer void of ZNF384-binding sequence (Panel A). Similar reporter gene assays were performed with *IL3* and *CSF2* promoters which do not have ZNF384 binding sites (Panel B) or in ALL cell lines Nalm6 (wtZNF384) and JIH5 (EPZ) (Panel C). Firefly luciferase activity was measured 24 hours post-transfection and normalized to Renilla luciferase activity. Relative luciferase activity indicates the ratio over the value from pGL3 basic vector alone. All experiments were performed in triplicate. Promoter, PR; enhancer, EN; wildtype *ZNF384*, wt*ZNF384*; *EP300-ZNF384* fusion, EPZ. Statistical significance was estimated for the comparison between EPZ and wtZNF384 using two-sided student *t*-test, with "n.s" signifying not significant ($P \geq 0.05$).

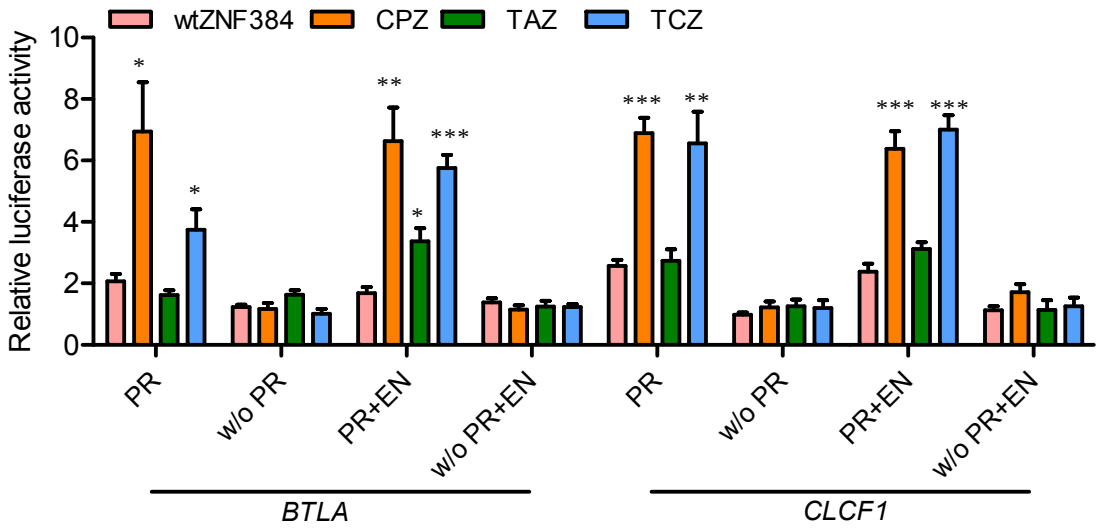

Supplemental Figure S7. *CREBBP-, TAF15-, and TCF3-ZNF384* fusions activated *CLCF1* and *BTLA* expression. HEK293T cells were transiently transfected with various combination of pGL3 luciferase construct, pcDNA *ZNF384* construct, and pGL-TK (Renilla luciferase). Luciferase constructs include luciferase gene downstream of *BTLA* or *CLCF1* promoter with or without ZNF384 binding sequence [PR or w/o PR], promoter plus enhancer with or without ZNF384 binding sequence [PR+EN or w/o PR+EN]). *ZNF384* constructs include insert of wildtype *ZNF384* (*wtZNF384*), *CREBBP-ZNF384* (CPZ), *TAF15-ZNF483* (TAZ), or *TCF3-ZNF384* (TCZ). Firefly luciferase activity was measured 24 hours post-transfection and normalized to Renilla luciferase activity. All experiments were performed in triplicate and repeated at least three times. Promoter, PR; enhancer, EN; *CREBBP-ZNF384* fusion, CPZ; *TAF15-ZNF384* fusion, TAZ; *TCF3-ZNF384* fusion, TCZ. Statistical significance was estimated for comparing ZNF384 fusion (CPZ, TAZ, or TCZ) against wt*ZNF384*, with *, **, *** signifying $P < 0.05$, < 0.01, < 0.001, respectively.

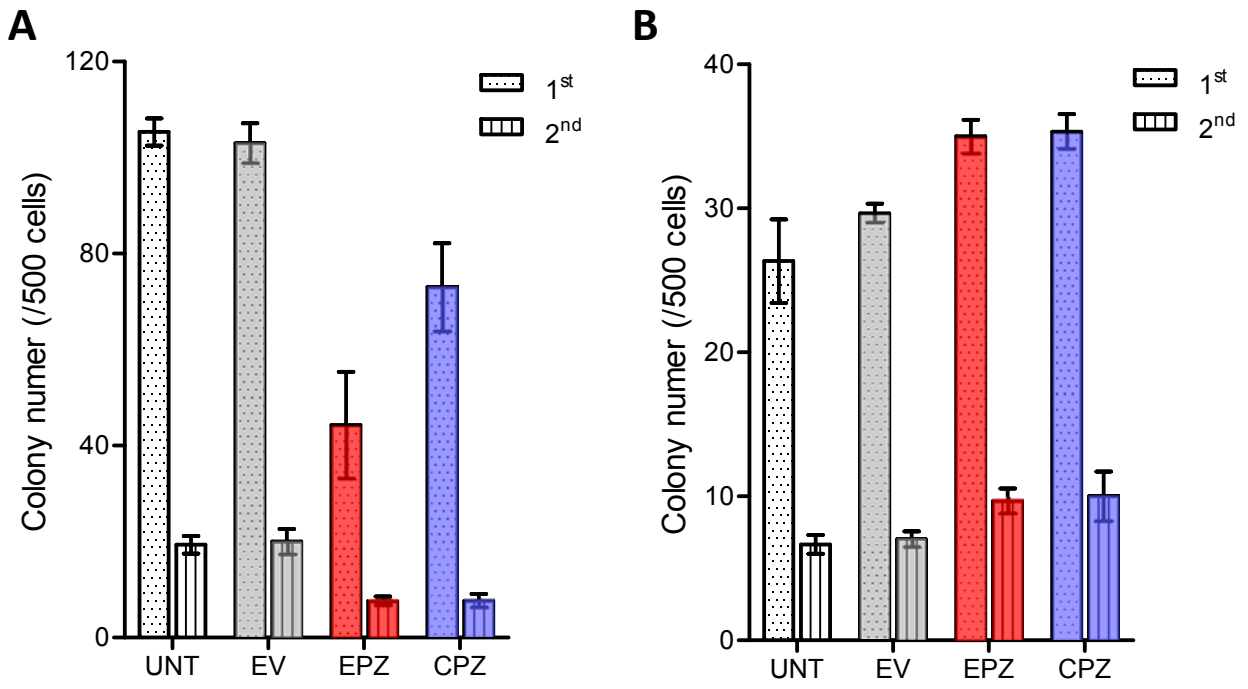

Supplemental Figure S8. *In vitro* replating potential of mouse hematopoietic stem and progenitor cells expressing *ZNF384* fusions. Lin$^-$Sca1$^+$c-Kit$^+$ cells were sorted from 8-10 weeks old CB57/BL6 mice by flow cytometry and lentivirally transduced with empty vector (EV), *EP300-ZNF384* (EPZ), or *CREBBP-ZNF384* (CPZ). Cells were then cultured in M3434 (**A**) and M3630 (**B**) methylcellulose medium (Stem Cell Technology), and colony number was counted 12-14 days later. Finally, cells were harvested and re-plated at the same density in M3434 (**A**) and M3630 (**B**) medium and colony formation of the second plating was assessed after 12-14 days.

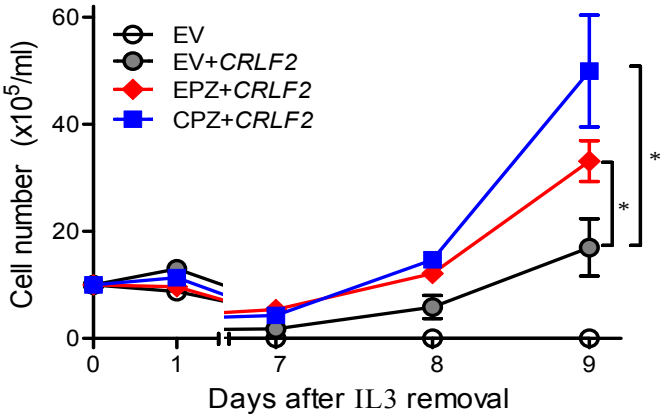

Supplemental Figure S9. *EP300-* and *CREBBP-NF384* fusions influenced hematopoietic progenitor cell transformation *in vitro.* Effects of fusion genes on Ba/f3 transformation. Following transduction of empty vector or *ZNF384* fusion genes with co-transduction of oncogenic *CRLF2*, Ba/f3 cells were cultured in IL3 depleted medium with cytokine-independent cell growth as a measure of oncogenic transformation. Number of viable cells was evaluated daily. All experiments were performed in triplicate and repeated twice. Empty vector, EV; *EP300-ZNF384* fusion, EPZ; *CREBBP-ZNF384* fusion, CPZ. Statistical significance of the differences between EPZ + *CRLF2* vs. EV + *CRLF2* or CPZ + *CRLF2* vs. EV + *CRLF2* were estimated by using two-way analysis of variance with * signifying $P < 0.05$.

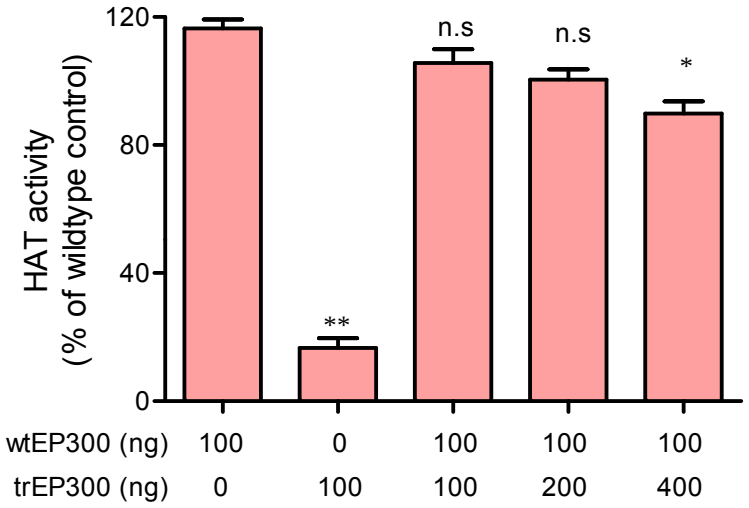

Supplemental Figure S10. Truncated EP300 lost HAT activity but without dominant negative effects. HAT enzymatic activity was measured for full length and truncated EP300 proteins. Proteins were expressed in Sf9 insect cells and purified to homogeneity. HAT activity was determined for each protein individually. Wildtype EP300 was mixed with increasing amount of truncated EP300 protein to examine dominate negative effects of the latter. Experiments were performed in triplicate and repeated twice. Statistical significance was estimated for comparison again the wtEP300 alone group, by using two-sided student *t*-test with n.s, * and ** signifying $P \geq 0.05$, < 0.05 and < 0.01, respectively.

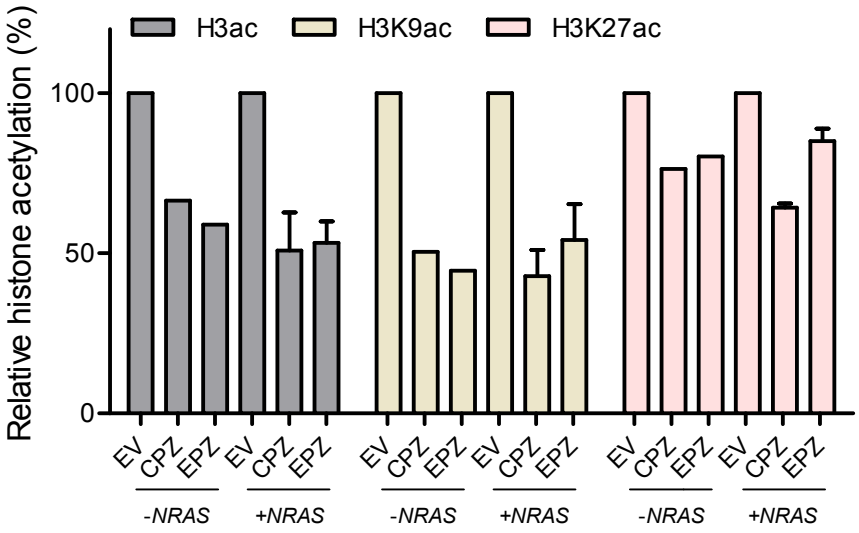

Supplemental Figure S11. *EP300-ZNF384* fusion resulted in global histone acetylation deregulation. Global H3, H3K9 and H3K27 acetylation were evaluated by western blot in Ba/f3 cells overexpressing *EP300-ZNF384* and *CREBBP-ZNF384* fusion, and the relative quantification of immunoblots were analyzed using Image Studio Lite version 4.0.21 (LI-COR Biosciences) and shown in bar graph. *EP300-ZNF384* fusion, EPZ; *CREBBP-ZNF384* fusion, CPZ; Empty vector, EV. The level of acetylated histone was first normalized to total H3 (loading control). Y axis represents normalized histone acetylation (total or K9-/K27-specific) relative to that of Ba/f3 cells transduced with EV.

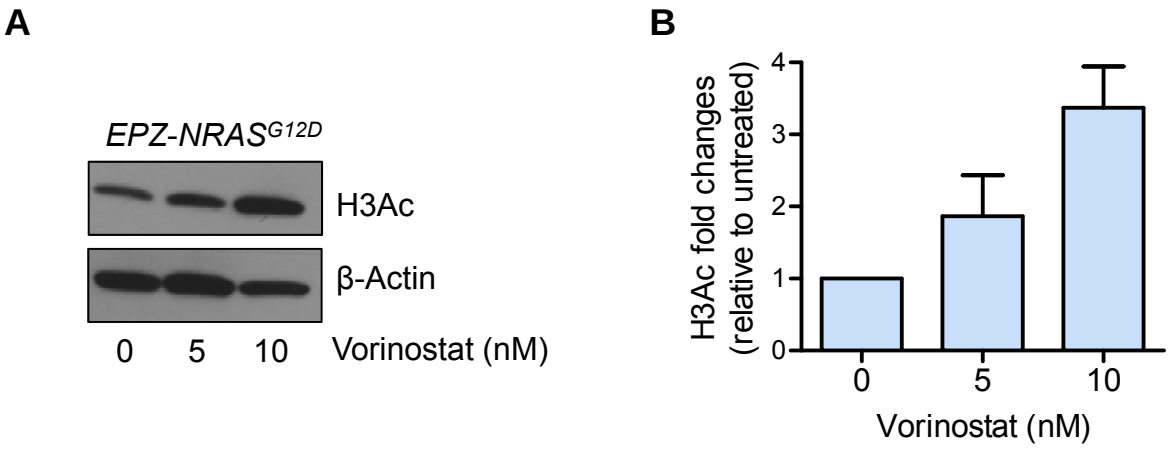

Supplemental Figure S12. Effects of Vorinostat on histone acetylation in Ba/f3 cells expressing *EP300-ZNF384*. (A) Global H3 acetylation was evaluated by western blot in *NRAS*^{G12D}-transformed Ba/f3 cells with ectopic *EP300-ZNF384* expression, with β-actin as a loading control. **(B)**The relative quantification of immunoblots were analyzed using Image Studio Lite version 4.0.21 (LI-COR Biosciences). Y axis represents normalized histone acetylation relative to untreated Ba/f3 cells.

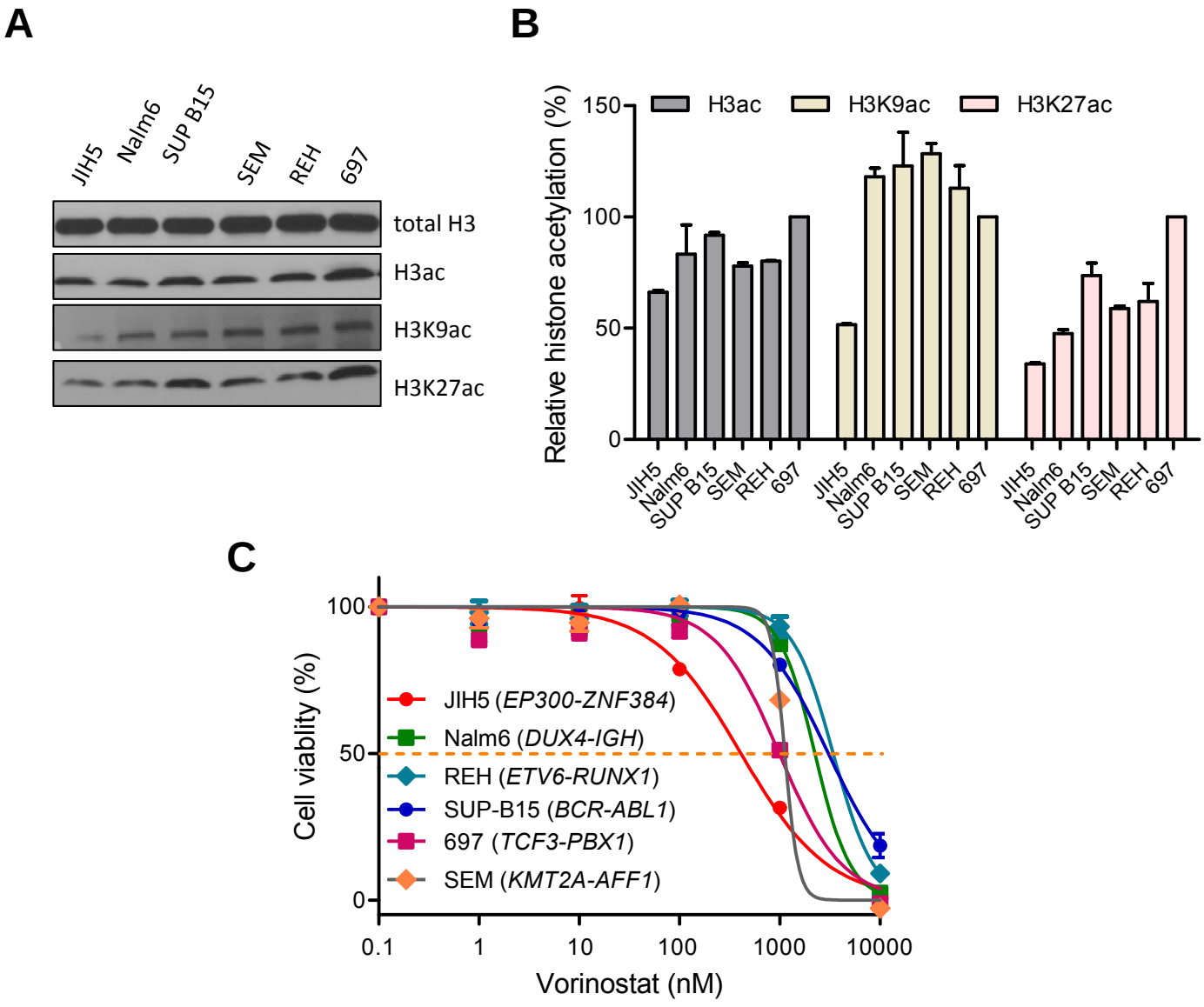

Supplemental Figure S13. *EP300-ZNF384* fusion resulted in global histone acetylation deregulation and increased sensitivity to HDAC inhibition. (A) Global H3, H3K9 and H3K27 acetylation were evaluated by western blot in 6 different ALL cell lines and the relative quantification of immunoblots were analyzed using Image Studio Lite version 4.0.21 (LI-COR Biosciences). **(B)** The level of acetylated histone was first normalized to total H3 (loading control). Y axis represents normalized histone acetylation (total or K9-/K27-specific) relative to that of 697 cells. **(C)** Cytotoxicity of HDAC inhibitor vorinostat was examined in *EP300-ZNF384* positive human ALL cell line JIH5 and cell lines Nalm6 (*DUX4-IGH*), REH (*ETV6-RUNX1*), SUP-B15 (*BCR-ABL1*), 697 (*TCF3-PBX1*) and SEM (*KMT2A-AFF1*), respectively. Cells were incubated with vorinostat for 48 hours and viability was then measured using MTT assay. Experiments were performed in triplicate and repeated three times. JIH5 was significantly more sensitive to vorinostat than any other ALL cell lines tested, as determined by two-way ANOVA ($P<0.05$).

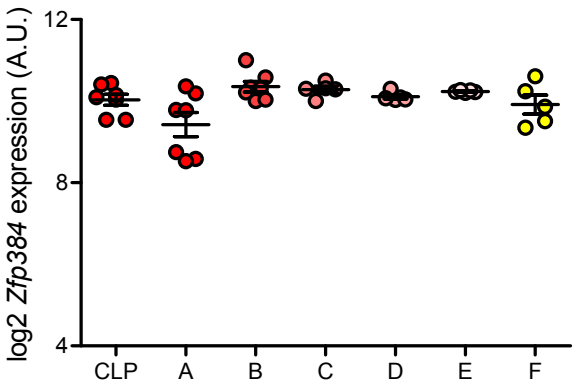

Supplemental Figure S14. Mouse *Znf384* gene expression during B cell differentiation. Expression value of *Zfp384* was extracted from a previously published dataset (GEO GSE38463) for mouse B-cells at different developmental stages. CLP (common lymphoid progenitor cell) is the most immature in this lineage, and Hardy fractions A-F represent gradual differentiation from ProB, PreB, to mature B cells.

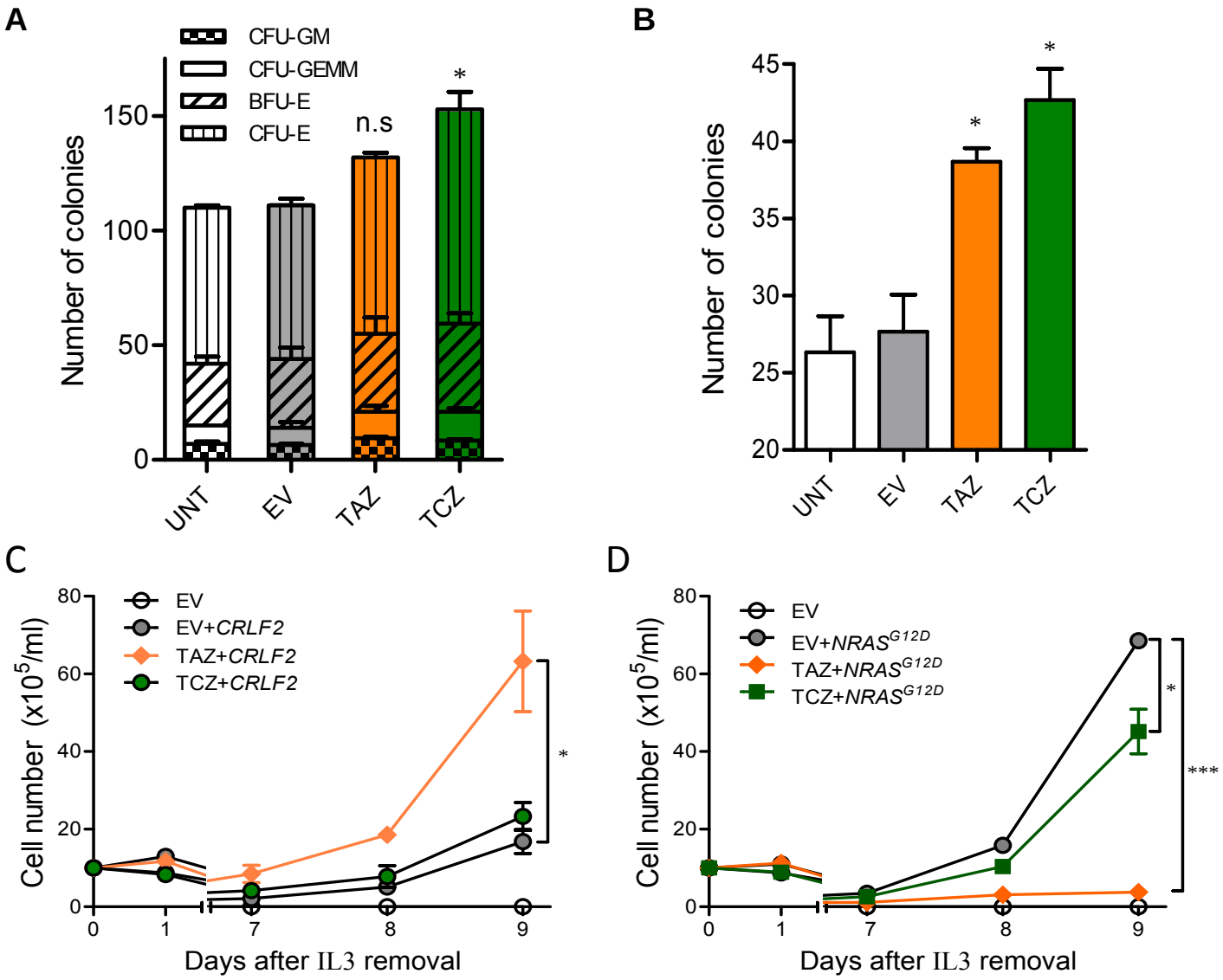

Supplemental Figure S15. *TAF15*- and *TCF3-ZNF384* fusions influenced hematopoiesis and hematopoietic progenitor cell transformation *in vitro.* (**A**-**B**) Effects of fusion genes on mouse hematopoiesis *in vitro*. Mouse Lin$^-$Sca1$^+$c-Kit$^+$ cells were lentivirally transduced with empty vector (grey), *TAF15-ZNF384* (orange), or *TCF3-ZNF384* fusion (green). Cells were then cultured in methylcellulose medium supplemented with cytokines for myelopoisis (Panel A) or preB cell differentiation (Panel B), and colonies formation was assessed 12-14 days later. (**C-D**) Effects of fusion genes on Ba/f3 transformation. Following transduction of empty vector, *TAF15-ZNF384 or TCF3-ZNF384* fusion with co-transduction of oncogenic *CRLF2* (C) *or NRAS^{G12D}* (D), Ba/f3 cells were cultured in IL3 depleted medium with cytokine-independent cell growth as a measure of transformation. Number of viable cells was evaluated daily. All experiments were performed in triplicate and repeated twice. Empty vector, EV; *TAF15-ZNF384* fusion, TAZ; *TCF3-ZNF384* fusion, TCZ; Colony-Forming Unit- Granulocyte, Macrophage, CFU-GM; Colony-Forming Unit-Granulocyte, Erythrocyte, Macrophage, Megakaryocyte, CFU-GEMM; Burst-Forming Unit-Erythroid, BFU-E; Colony-Forming Unit-Erythroid, CFU-E. Statistical significance was estimated for comparison against the EV group unless otherwise indicated, by using two-way analysis of variance with n.s, *, *** signifying $P \geq 0.05$, < 0.05 and < 0.001, respectively.

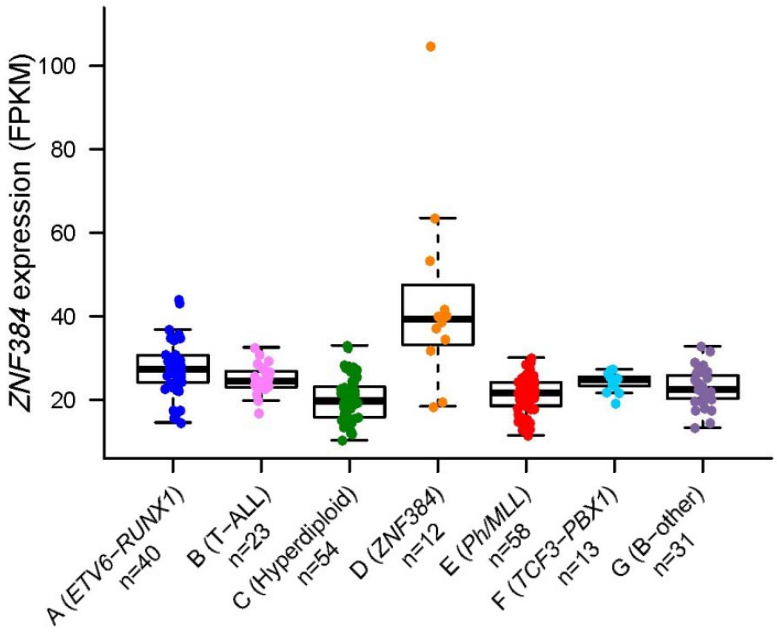

Supplemental Figure S16. *ZNF384* gene expression in the ALL subgroups. Expression of the *ZNF384* gene in 7 ALL subgroups identified from hierarchical clustering. Each sample is represented by a dot and is color-coded according to the subgroups it belongs to.

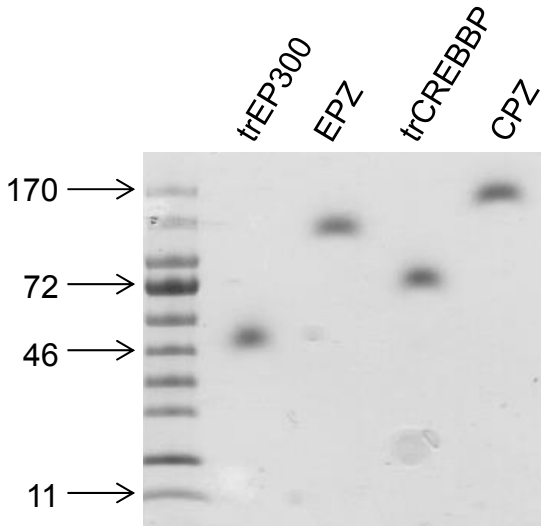

Supplemental Figure S17. Coomassie Brilliant Blue staining of purified fusion or truncated EP300 and CREBBP proteins. Protein expression and purification were described in Methods. A total of 100ng of respective proteins were loaded on SDS-PAGE gel and subjected to electrophoresis, followed by Coomassie Brilliant Blue staining according to standard procedures. truncated EP300, trEP300; truncated CREBBP, trCREBBP; *EP300-ZNF384* fusion, EPZ; *CREBBP-ZNF384* fusion, CPZ;